arXiv:1604.08584v2 [gr-qc] 7 May 2016

Black Hole Remnants in Hayward Solutions and Noncommutative Effects

S. H. Mehdipour[a,*] and **M. H. Ahmadi**[a,†]

[a] *Department of Physics, College of Basic Sciences, Lahijan Branch, Islamic Azad University, P. O. Box 1616, Lahijan, Iran*

Abstract

In this paper, we explore the final stages of the black hole evaporation for Hayward solutions. Our results show that the behavior of Hawking's radiation changes considerably at the small radii regime such that the black hole does not evaporate completely and a stable remnant is left. We analyse the effect that an inspired model of the noncommutativity of spacetime can have on the thermodynamics of Hayward spacetimes. This has been done by applying the noncommutative effects to the non-rotating and rotating Hayward black holes. In this setup, all point structures get replaced by smeared distributions owing to this inspired approach. The noncommutative effects result in a colder black hole in the small radii regime as Hayward's free parameter g increases. As well as the effects of noncommutativity and the rotation factor, the configuration of the remnant can be substantially affected by the parameter g. However, in the rotating solution it is not so sensitive to g with respect to the non-rotating case. As a consequence, the noncommutativity and the rotation may raise the minimum value of energy for the possible formation of black holes in TeV-scale collisions. This observation can be used as a potential explanation for the absence of black holes in the current energy scales produced at particle colliders.

Key Words: Regular Black Holes, Hawking Temperature, Noncommutative Geometry, Black Hole Remnant

*mehdipour@liau.ac.ir

† ahmadi@liau.ac.ir

1 Introduction

Black holes (BHs) and singularities are accepted to be unavoidable predictions of the theory of general relativity [1]. It is widely believed that only a not yet attainable quantum gravity theory would be capable to study the issue of central singularity of a BH properly. However, various phenomenological approaches have been considered in the literature in order to solve the problem of BH's singularity with a regular center [2]. The Bardeen BH [3] is the first regular model which has proposed as a spherically symmetric compact object with an event horizon and without violating the weak energy condition. The inside of its horizon is deSitter-like wherein the matter has a high pressure. In 2006, the formation and evaporation of a new kind of regular solutions was studied by Hayward [4]. The static region of a Hayward spacetime is Bardeen-like while the dynamic regions are Vaidya-like. A general class of regular solutions utilizing a mass function that generalizes the Bardeen and Hayward mass terms have been suggested [5]. The authors of Ref. [6] have discussed the massive scalar quasinormal modes of the Hayward BH (H-BH). The motion of a particle in background of a H-BH has been studied [7]. The accretion of fluid flow around the modified H-BH has been investigated [8]. Recently, the effects of thermal fluctuations on thermodynamics of a modified H-BH have also been analyzed [9]. There have been a great number of studies concerning regular BHs in the recent literature [10-14].

On the other hand, the appearance of high energies in a noncommutative manifold is a consequence of quantum fluctuation effects at very short distances wherein any measurements to determine a particle position with an accuracy more than an innate minimal length scale, namely the Planck length, are hindered. Noncommutative BHs are naturally identified with the possible running of this minimal length scale in BH physics. Based on an inspired noncommutative model [15-19], instead of describing a point particle as a Dirac-delta function distribution, it is characterized by a Gaussian function distribution with a minimal width $\sqrt{\theta}$, i.e. a smeared particle, where θ is the smallest fundamental cell of an observable area in the noncommutative spacetime, beyond which coordinate resolution is not obvious. In this model, the energy-momentum tensor takes a new form, while the Einstein tensor remains unchanged. As an important result, the curvature singularity at the center of a noncommutative BH is eliminated. This means that Planck scale physics may prevent the appearance of a singularity in the center of a BH wherein a BH remnant may be formed (for an extensive review of BH remnants, see [20]).

In the group of various BH solutions, the rotating ones, without any hesitations, are most suitable to fit the observational data proving that collapsed objects display high angular momenta. The BH spin plays a fundamental role in any astrophysical process. Hence, its perfect comprehension is essential for the exact explanation of astrophysical

BHs. Furthermore, the astrophysical BHs might be inherently quantum objects, macroscopically different from the rotating ones predicted in Einstein's theory of gravity. It turns out to be a rather long process to solve Einstein's vacuum equations directly for a rotating solution. Instead, by describing a trick of Newman and Janis [21], one can obtain, for example, the Kerr solution from the Schwarzschild case. The same trick can then be applied to a regular case to achieve a rotating regular solution. In 2013, Bambi and Modesto [22] apply the Newman-Janis algorithm to the Hayward and to the Bardeen metrics to obtain a family of rotating regular BHs.

In this paper, we first consider the most popular model of a regular BH derived in [4], namely the H-BH, and then study its radiating behavior and the resulting remnant by providing its Hawking temperature. We compare different sizes of remnants with the noncommutative ones by including the noncommutative corrections in the line element of H-BH, i.e. the Noncommutative H-BH (NH-BH). Finally, using the Newman-Janis algorithm which is often remarked as a short cut to find spinning BH solutions via the corresponding non-rotating ones, we consider again the inspired noncommutativity and determine the Hawking temperature of the Noncommutative Rotating H-BH (NRH-BH). Throughout the paper, natural units are used, i.e. $\hbar = c = G = k_B = 1$ and Greek indices run from 0 to 3.

2 Hayward solution

The H-BH solution obtained by Hayward [4] is given by the following metric,

$$ds^2 = N(r)dt^2 - N^{-1}(r)dr^2 - r^2 d\Omega^2, \tag{1}$$

with

$$N(r) = 1 - \frac{2m(r)}{r} = 1 - \frac{2Mr^2}{r^3 + g^3}. \tag{2}$$

where g is a real free parameter and shows a positive constant measuring the deviations from the standard Kerr spacetime. In the above, the mass term $m(r) = Mr^3/(r^3+g^3)$ may show the mass inside the sphere of radius r such that in the limit $r \to \infty$ it approaches the BH mass M. This solution is everywhere nonsingular and the weak energy condition is not violated. The emitted feature of such a regular BH can now be simply analysed by displaying the temporal component of the metric as a function of radius for an extremal H-BH with different values of g. This has been presented in Fig. (1). This figure exhibits the possibility of having an extremal configuration with one degenerate event horizon at a minimal nonzero mass M_0. In fact, the condition for having one degenerate event horizon is that $M = M_0$ which means for $M < M_0$ there is no event horizon. The existence of

a minimal nonzero mass may be interpreted as the deSitter-like region corresponding to the interior of the horizon which yields a remnant that the H-BH may shrink to.

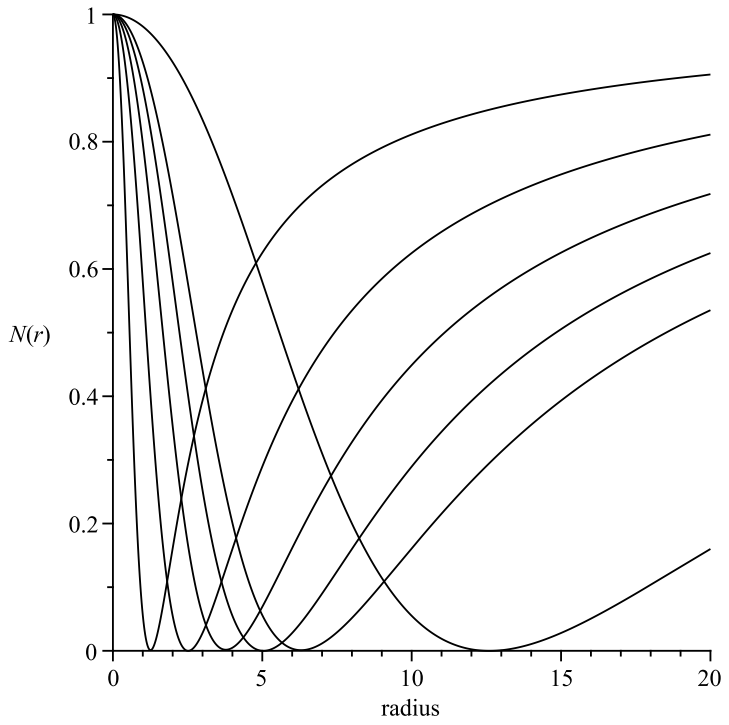

Figure 1: The temporal component of the metric, $N(r)$, in terms of the radius r for different values of g. The figure displays the possibility of having extremal configuration with one degenerate event horizon at a minimal nonzero mass M_0. This presents the existence of M_0 such that the H-BH may shrink to. On the right-hand side of the figure, from top to bottom, the solid lines correspond to the H-BH for $g = 1.00,\ 2.00,\ 3.00,\ 4.00,\ 5.00$, and $g = 10.00$, respectively.

The horizon radius of the H-BH can be obtained by the real positive root of the following equation,

$$r_H^3 - 2Mr_H^2 + g^3 = 0. \tag{3}$$

So, one can find the H-BH mass in terms of r_H as follows:

$$M = \frac{r_H^3 + g^3}{2r_H^2}. \tag{4}$$

The numerical results of the mass versus the radius are presented in Fig. 2. As can be seen from Fig. (2), the minimal nonzero mass increases as the parameter g increases. The regularity at very short distances of the H-BH spacetime implies a remnant mass corresponding to a remnant radius r_0. Here we have shown that the final stage of the evaporation of H-BH is a remnant in which it has an increasing size with raising its own free parameter.

When such a regular BH radiates, its temperature is given by

$$T_H = \frac{1}{4\pi}\frac{dN(r)}{dr}\Big|_{r=r_H} = \frac{Mr_H(r_H^3 - 2g^3)}{2\pi(r_H^3 + g^3)^2}. \tag{5}$$

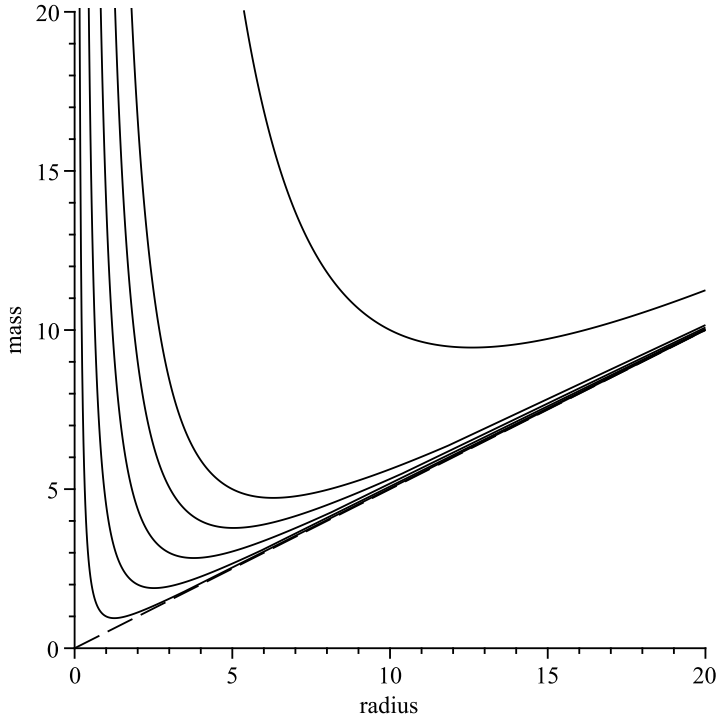

Figure 2: The mass of the H-BH as a function of the horizon radius for different values of g. On the left-hand side of the figure, from left to right, the solid lines correspond to the H-BH for $g = 1.00,\ 2.00,\ 3.00,\ 4.00,\ 5.00$, and $g = 10.00$, respectively. The dashed line refers to the Schwarzschild case so that it corresponds to $g = 0$.

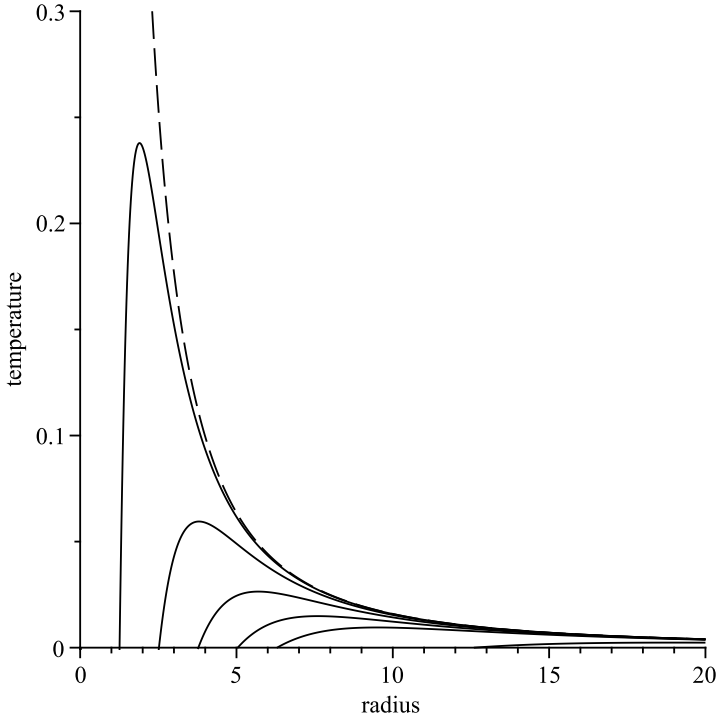

Figure 3: The Hawking temperature versus the horizon radius. We have set $M = 10.00$. On the left-hand side of the figure, from left to right, the solid lines correspond to the H-BH for $g = 1.00,\ 2.00,\ 3.00,\ 4.00,\ 5.00$, and $g = 10.00$, respectively. The dashed line refers to the Schwarzschild case so that it corresponds to $g = 0$.

Table 1: The remnant mass, the remnant radius and also the maximum temperature of the H-BH for different values of g. As the parameter g increases the size and the mass of the H-BH remnant increase but the maximum temperature decreases. For a large amount of g, i.e. $g \gg 1$, there is a linear relationship between the remnant mass and the remnant radius. As can be seen from the table, the results are confirmed by the numerical results of Figs. 1, 2 and 3.

H-BH			
Free Parameter	Remnant Mass	Remnant Radius	Maximum Temperature
$g = 1.00$	$M_0 \approx 0.94$	$r_0 \approx 1.26$	$T_H(max) \approx 0.238$
$g = 2.00$	$M_0 \approx 1.89$	$r_0 \approx 2.52$	$T_H(max) \approx 0.059$
$g = 3.00$	$M_0 \approx 2.83$	$r_0 \approx 3.78$	$T_H(max) \approx 0.026$
$g = 4.00$	$M_0 \approx 3.78$	$r_0 \approx 5.04$	$T_H(max) \approx 0.015$
$g = 5.00$	$M_0 \approx 4.72$	$r_0 \approx 6.30$	$T_H(max) \approx 0.009$
$g = 10.00$	$M_0 \approx 9.45$	$r_0 \approx 12.60$	$T_H(max) \approx 0.002$

Due to the emission of Hawking radiation, the Hawking temperature finally reaches a peak at the final stage of the evaporation and then abruptly drops to zero so that a stable remnant is appeared. The numerical result of the Hawking temperature in terms of the horizon radius is displayed in Fig. 3. According to Fig. 3, the temperature peak of the H-BH decreases as the parameter g increases, so a H-BH for a larger amount of g is colder and its remnant is bigger. If we set $g = 0$, so the Hawking temperature for the Schwarzschild BH, i.e. $T_H = M/(2\pi r_H^2)$, which is accompanied by a divergence at $M = 0$ is retrieved.

Table 1, for further specifications of the H-BH remnant, shows the numerical results of the remnant size, the remnant mass and also the maximum temperature for different values of g. In accordance with Table 1, as g becomes larger both the minimal mass and the minimal radius get larger but the temperature peak becomes smaller. In the limit $g \gg 1$, the free parameter g is proportional to the remnant mass and to the remnant radius, i.e. $g \propto M_0 \propto r_0$. In other words, for an adequately large amount of g which corresponds to a large radius, there is a linear relationship between the minimal mass and the minimal radius which is similar to the result appeared in the relationship between the horizon radius and the BH mass for the Schwarzschild BH.

3 Noncommutative Hayward solution

Our strategy here is that, firstly, the noncommutativity influences on the spacetime of non-rotating Hayward are investigated and the thermodynamics features of the NH-BH are determined. Afterwards, in the later section, taking into account the Newman-Janis

algorithm, we apply the inspired noncommutativity and recompute the Hawking temperature of the NRH-BH.

In accord with [23], the Newman-Janis algorithm works only for vacuum solutions but the authors in [24] have presented a new prescription that comprises the case of non-vanishing stress tensors. As an introduction of the idea, let us begin by the Schwarzschild-like form of spacetimes which explain the line elements in the so-called Kerr-Schild classification and in the presence of matter

$$ds^2 = ds_M^2 - \frac{h(r)}{r^2}\left(n_\alpha dx^\alpha\right)^2, \tag{6}$$

where the expression ds_M^2 is the Minkowski metric in a spherical basis and n_α is a null vector in the coordinates of Minkowski. The function $h(r)$ can be written as

$$h(r) = 2m(r)r. \tag{7}$$

In accordance with the Kerr-Schild decomposition, Eq. (7) has a generic validity, thus its general form is unchanged and it is not sensitive to various structures of the mass term. The expression $h(r)$ for the H-BH metric is given by

$$h(r) = \frac{2Mr^4}{r^3 + g^3}. \tag{8}$$

Here, we apply the inspired noncommutative methodology [15-19] (see also [25]). According to this method, the point-like structure of mass, instead of being entirely localized at a point, is characterized by a smeared structure throughout a region of linear size $\sqrt{\theta}$. This means that the mass density of a static, spherically symmetric, particle-like gravitational source cannot be a delta function distribution, but will be found to be a Gaussian distribution

$$\rho_\theta(r) = \frac{M}{(4\pi\theta)^{3/2}} e^{-\frac{r^2}{4\theta}}. \tag{9}$$

The smeared mass distribution can implicity be written in terms of the lower incomplete Gamma function,

$$M_\theta = \int_0^r \rho_\theta(r) 4\pi r^2 dr = \frac{2M}{\sqrt{\pi}}\gamma\Big(\frac{3}{2}; \frac{r^2}{4\theta}\Big). \tag{10}$$

The resulting metric describing the NH-BH is given by Eq. (1), with the following $m(r)$ in terms of the smeared mass distribution M_θ

$$m(r) = M_\theta\left(\frac{r^3}{r^3 + g^3}\right). \tag{11}$$

The thermodynamics description of the NH-BH can now be simply analysed by displaying the temporal component of the metric versus the radius for an extremal BH with different values of g which has been presented in Fig. (4)[‡].

[‡]For simplicity of numerical calculations, we assume $\theta = 1$.

It is clear that the metric of the NH-BH has a coordinate singularity at the event horizon as

$$r_H = 2m(r_H), \tag{12}$$

with

$$m(r_H) = \frac{2M}{\sqrt{\pi}} \left(\frac{r_H^3}{r_H^3 + g^3} \right) \gamma\Big(\frac{3}{2}; \frac{r_H^2}{4\theta}\Big). \tag{13}$$

The analytical solution of Eq. (12) for the horizon radius in a closed form is not feasible, but one can solve it to obtain M, which gives the mass of the NH-BH in terms of r_H. We find

$$M = \frac{r_H^3 + g^3}{2r_H^2 \left[\mathcal{E}\left(\frac{r_H}{2\sqrt{\theta}}\right) - \frac{r_H}{\sqrt{\pi\theta}} e^{-\frac{r_H^2}{4\theta}} \right]}, \tag{14}$$

where $\mathcal{E}(n)$ is the Gaussian error function defined as $\mathcal{E}(n) \equiv 2/\sqrt{\pi} \int_0^n e^{-x^2} dx$. In the limit $\theta \to 0$, the Gaussian error function is equal to one and the exponential term is reduced to zero, thus we recover Eq. (4). In other words, if $\sqrt{\theta}$ is too small, the background geometry is interpreted as a smooth differential manifold and the smeared-like mass descends to the point-like mass. However, in the regime that noncommutative fluctuations are important, $r \to \sqrt{\theta}$, the microstructure of spacetime deviates considerably from the macroscopic one and provides new physics at very short distances.

The results of the numerical solution of the mass as a function of the horizon radius are displayed in Fig. 5. According to the numerical results it is concluded that the noncommutative version of the mass equation (14), leads to a bigger minimal nonzero mass at small radii in comparison with the standard commutative version.

The Hawking temperature of the NH-BH can be written as

$$T_H = \frac{1}{4\pi} \frac{dN(r)}{dr}\Big|_{r=r_H} = \frac{M}{4\sqrt{(\pi\theta)^3}\,(r_H^3 + g^3)^2} \Big[4r_H \sqrt{\pi\theta^3} \left(\frac{r_H^3}{2} - g^3 \right) \mathcal{E}\left(\frac{r_H}{2\sqrt{\theta}} \right) - r_H^2 e^{-\frac{r_H^2}{4\theta}} \left(r_H^5 + 2r_H^3\theta + r_H^2 g^3 - 4\theta g^3 \right) \Big]. \tag{15}$$

In the commutative version and for $g = 0$, the Gauss error function is equal to one and the exponential term is zero, so we retrieve the Hawking temperature of a Schwarzschild BH. The numerical result of the NH-BH temperature in terms of the horizon radius is shown in Fig. 6. From the figure we see that the maximum temperature decreases with raising the parameter g. As a result, the size and the mass of the NH-BH remnant at the ultimate phase of the evaporation is bigger in comparison with the noncommutative Schwarzschild one.

For more specifications, we present Table 2 that is similar to Table 1. From Table 2 we see that as g grows both the remnant mass and the remnant radius are increased which

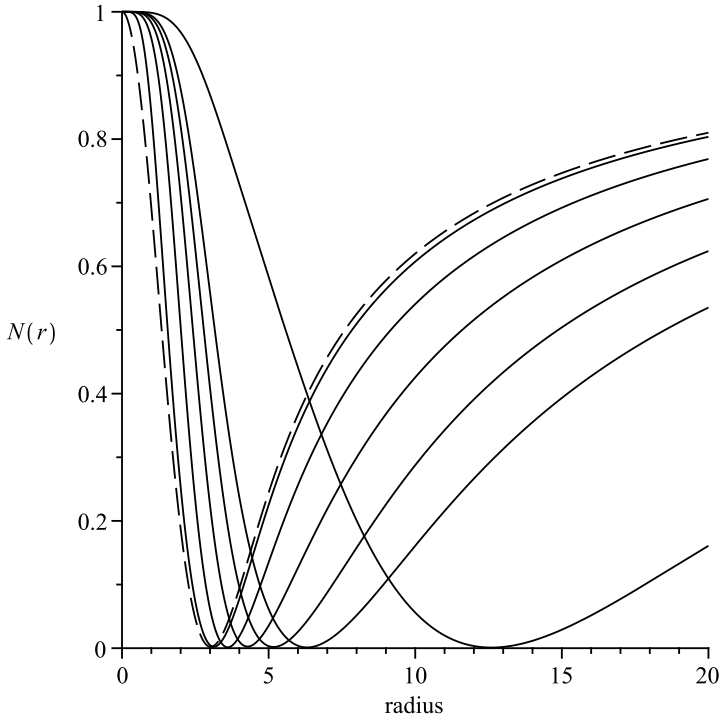

Figure 4: The temporal component of the metric, versus the radius for different values of g. The figure shows the possibility of having extremal configuration with one degenerate event horizon at $M = M_0$ (extremal NH-BH). This shows the existence of a minimal non-zero mass that the black hole can shrink to. On the right-hand side of the figure, from top to bottom, the solid lines correspond to the NH-BH for $g = 1.00,\ 2.00,\ 3.00,\ 4.00,\ 5.00$, and $g = 10.00$, respectively. The dashed line refers to the Schwarzschild case so that it corresponds to $g = 0$.

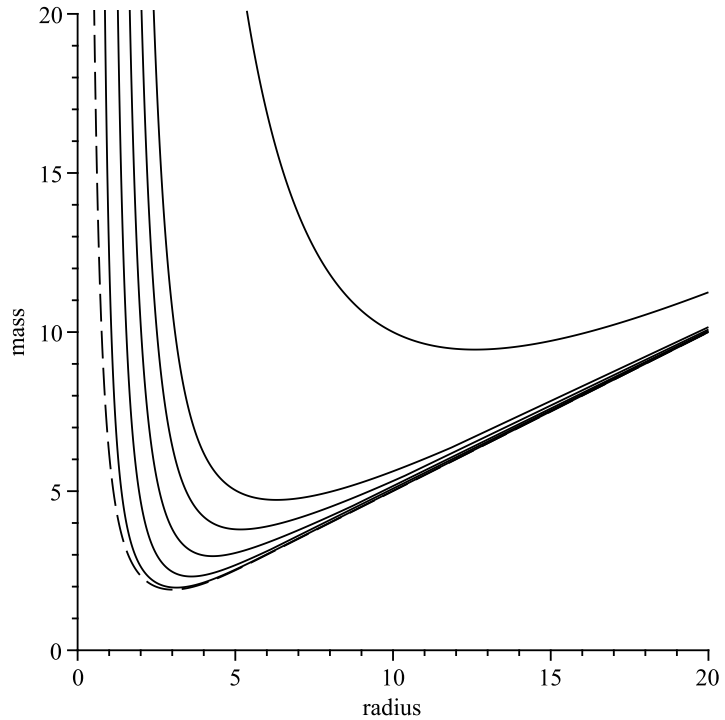

Figure 5: The mass of the NH-BH versus the horizon radius for different values of g. On the left-hand side of the figure, from left to right, the solid lines correspond to the NH-BH for $g = 1.00,\ 2.00,\ 3.00,\ 4.00,\ 5.00$, and $g = 10.00$, respectively. The dashed line refers to the Schwarzschild case so that it corresponds to $g = 0$.

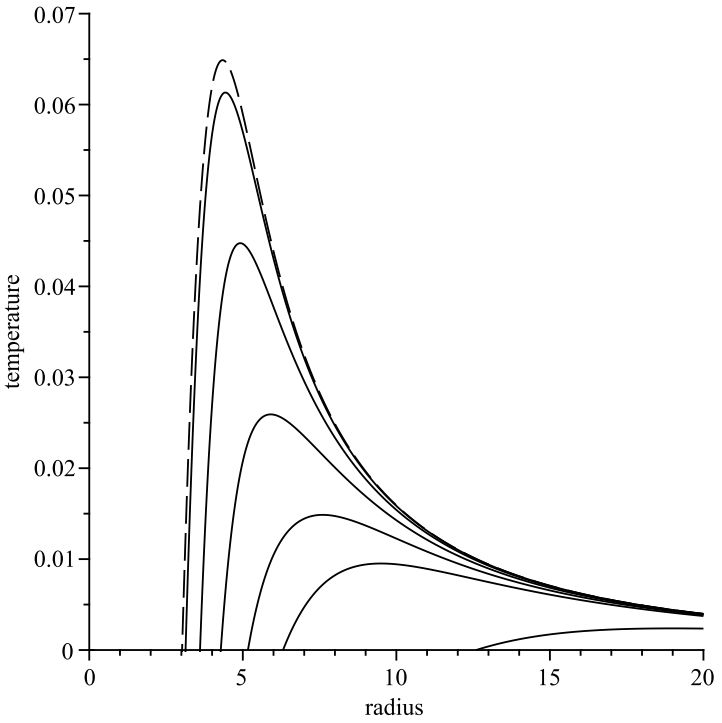

Figure 6: The Hawking temperature versus the horizon radius. We have set $M = 10.00$. On the left-hand side of the figure, from left to right, the solid lines correspond to the NH-BH for $g = 1.00,\ 2.00,\ 3.00,\ 4.00,\ 5.00$, and $g = 10.00$, respectively. The dashed line refers to the Schwarzschild case so that it corresponds to $g = 0$.

finally, in the limit $g \gg 1$, yields a proportional relationship $g \propto M_0 \propto r_0$. A comparison between the final stages of the evaporation for the noncommutative Schwarzschild BH and the NH-BH shows that raising the size and the mass of the remnant and also getting a colder BH is affected by an increase in the parameter g. In addition, as can be seen from Figs. (4), (5), (6) and Table 2 the noncommutative coordinates yields a bigger remnant and also a colder BH at small radii compared to its commutative case.

As an important note the thermodynamics descriptions of such noncommutative regular BHs are substantially similar to that of the framework of gravity's rainbow [26]. According to our results the minimum required energy for the formation of such a BH at particle colliders such as LHC will be larger. This is in agreement with the results obtained in the context of gravity's rainbow [27]. In Ref. [27], the remnant mass has found to be greater than the energy scale at which experiments were performed at the LHC. They have proposed this as a possible explanation for the absence of BHs at the LHC. In addition, the authors in Ref. [28] have found that a remnant depends critically on the structure of the rainbow functions [29]. They have argued that, using the framework of gravity's rainbow, a remnant is formed for all black objects in such a way that it is a model-independent phenomenon.

It may be noted that as another striking example of regular black holes, if the Bardeen solution is chosen, solely the mass term will be changed, however the general properties

Table 2: The table in the upper place shows the remnant mass, the remnant radius and the maximum temperature of the noncommutative Schwarzschild BH, while the table below shows them for the NH-BH with different values of g.

Noncommutative Schwarzschild BH		
Remnant Mass	Remnant Radius	Maximum Temperature
$M_0 \approx 1.90$	$r_0 \approx 3.02$	$T_H(max) \approx 0.065$

NH-BH			
Free Parameter	Remnant Mass	Remnant Radius	Maximum Temperature
$g = 1.00$	$M_0 \approx 1.96$	$r_0 \approx 3.13$	$T_H(max) \approx 0.062$
$g = 2.00$	$M_0 \approx 2.31$	$r_0 \approx 3.60$	$T_H(max) \approx 0.045$
$g = 3.00$	$M_0 \approx 2.95$	$r_0 \approx 4.28$	$T_H(max) \approx 0.026$
$g = 4.00$	$M_0 \approx 3.79$	$r_0 \approx 5.16$	$T_H(max) \approx 0.015$
$g = 5.00$	$M_0 \approx 4.72$	$r_0 \approx 6.31$	$T_H(max) \approx 0.009$
$g = 10.00$	$M_0 \approx 9.45$	$r_0 \approx 12.60$	$T_H(max) \approx 0.002$

will be directed to entirely comparable consequences to those above [30].

4 Noncommutative rotating Hayward solution

For spinning solution, we apply the Newman-Janis algorithm, and assuming that the mass term $m(r)$ is not affected by the complexification $r \to r' = r + ia\cos\vartheta$, the general form of the Kerr-Schild decomposition (6) holds

$$ds^2 = ds^2_M - \frac{h(r)}{r'\bar{r}'}\left(n_\alpha dx^\alpha\right)^2, \tag{16}$$

where n_α is written in spheroidal coordinates and $h(r)$ is unaltered by expressing $m(r')$ as $m(\mathrm{Re}(r')) = m(r)$. In fact, even with changing the symmetry from a spherically symmetric geometry to an axially symmetric geometry, the formal structure of the Kerr-Schild solution does not change. This is consistent with the solution of type-I or the first-class solution of the RH-BH in [22], i.e. the complexification of the $1/r$ term as in Schwarzschild, without changing the mass term.

Now, with the above explanation, one can obtain the line element of RNH-BH in Boyer-Lindquist coordinates

$$\begin{aligned} ds^2 = \frac{\Delta - a^2\sin^2\vartheta}{\Sigma}dt^2 - \frac{\Sigma}{\Delta}dr^2 - \Sigma d\vartheta^2 + 2a\sin^2\vartheta\left(1 - \frac{\Delta - a^2\sin^2\vartheta}{\Sigma}\right)dtd\phi \\ - \sin^2\vartheta\left[\Sigma + a^2\sin^2\vartheta\left(2 - \frac{\Delta - a^2\sin^2\vartheta}{\Sigma}\right)\right]d\phi^2, \end{aligned} \tag{17}$$

where $\Delta := r^2 - 2m(r)r + a^2$ (with $m(r)$ given by Eq. (11)) and $\Sigma := r^2 + a^2\cos^2\vartheta$.

The Hawking temperature of the NRH-BH is then found to be

$$T_H = \frac{1}{4\pi(r_+^2+a^2)}\frac{d\Delta}{dr}\bigg|_{r=r_+} = -\frac{1}{4\sqrt{(\pi\theta)^3}(r_+^3+g^3)^2(r_+^2+a^2)}\Big[8\sqrt{\pi\theta^3}Mr_+^3\left(\frac{r_+^3}{4}+g^3\right)\mathcal{E}\left(\frac{r_+}{2\sqrt{\theta}}\right)$$

$$+\left(Mr_+^9 - 2M\theta r_+^7 + Mg^3r_+^6 - 8M\theta g^3 r_+^4\right)e^{-\frac{r_+^2}{4\theta}} - 2\sqrt{\pi\theta^3}r_+(r_++g)^2(r_+^2-gr_++g^2)^2\Big]. \quad (18)$$

Note that, for the commutative case and for $g = a = 0$, the function $\mathcal{E}(r_+/2\sqrt{\theta})$ becomes one and the exponential term is zero, but the last term in Eq. (18) which is independent of the mass M will be reduced to $1/(2\pi r_+)$. Hence, one retrieves the standard result

$$T_H = -\frac{M}{2\pi r_+^2} + \frac{1}{2\pi r_+} = \frac{1}{4\pi r_+}, \quad (19)$$

where in this case $r_+ = r_H = 2M$. Finally, the numerical result of the Hawking temperature as a function of the outer horizon radius (Eq. (18)) is shown in Fig. 7. In accord with the figure, the size and the mass of the NRH-BH remnant at the final stage of the evaporation increase with increasing the parameter g. However, in the rotating case it is not so sensitive to g with respect to the non-rotating one.

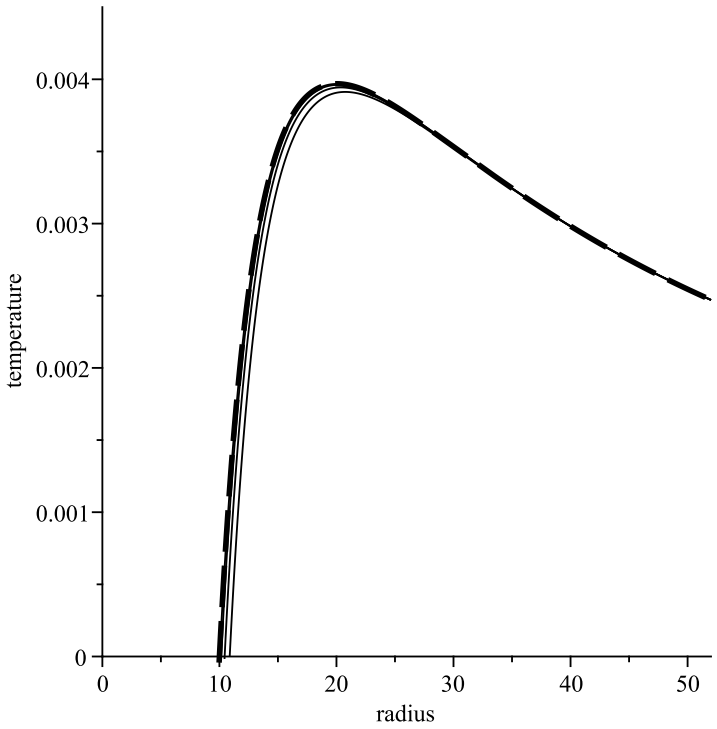

Figure 7: The temperature T_H versus the outer horizon radius, r_+. We have set $M = 10.00$ and $a = 1.00$. On the left-hand side of the figure, from left to right, the solid lines correspond to the NRH-BH for $g = 1.00,\ 2.00,\ 3.00,\ 4.00,\ 5.00$, and $g = 10.00$, respectively. The dashed line refers to the noncommutative Kerr BH so that it corresponds to $g = 0$. It is clear that the curves are not so sensitive to g.

In order to compare the noncommutative results with the commutative case ($\theta \to 0$), we display the plot for the temperature of the RH-BH as a function of r_+ (see Fig. 8). One can see that the noncommutative effects are caused to have a larger size and mass of the remnant in addition to a colder BH. Furthermore, it is reasonable to expect that the enlarging the amounts of the remnant mass is the role of the rotation as well.

Generally, in Figs. 7 and 8, we see that the feature of the temperature is nearly similar to that of the nonrotating case. After a temperature peak, the NRH-BH calms down to a zero temperature as a NRH-BH remnant at the final phase of its evaporation. The size and the mass of this remnant becomes larger with respect to the nonrotating solution and this is due to the fact that the rotational kinetic energy is kept in the final format. As a consequence, the noncommutative effects and the rotation factor can raise the minimum value of energy for the possible production of BHs in TeV-scale collisions at particle colliders. Thus, the possibility for the formation and detection of BHs will be reduced.

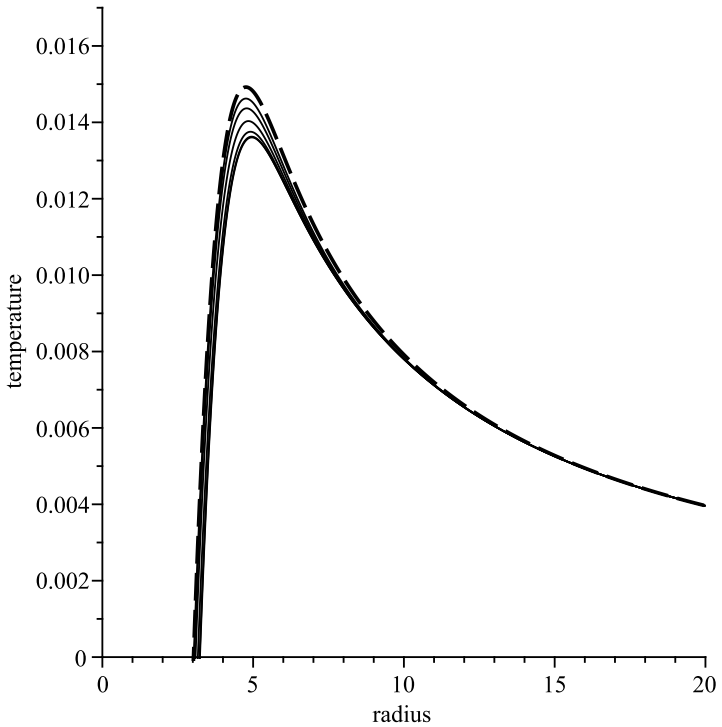

Figure 8: The temperature T_H versus the outer horizon radius, r_+. We have set $M = 10.00$ and $a = 1.00$. The solid lines through the center of the figure, from top to bottom, correspond to the RH-BH for $g = 1.00,\ 2.00,\ 3.00,\ 4.00,\ 5.00,$ and $g = 10.00$, respectively. The dashed line refers to the Kerr BH so that it corresponds to $g = 0$.

5 Conclusions

We have proposed that the final phase of the BH evaporation is a stable remnant. In this study, the H-BH as a most popular model of regular BHs has been chosen. The thermodynamics features of its non-rotating and rotating solution in the presence of an inspired model of noncommutative geometry have been analysed. The effect of this inspired noncommutativity in the microscopic feature of spacetime is that all point structures are replaced by structures smeared via such an inspired microstructure. We have explored the effect that the deformation of a point mass has on the thermodynamics of H-BH solutions. Thus, the corrections to the Hawking temperature via such a modification of the theory have been found. Finally we have extended our analysis to the thermodynamic properties of noncommutative spinning solutions, providing their Hawking temperature. It is concluded that, the noncommutative effects cause an increasing size and mass of the remnant and also making the BH to be colder in the small radii regime as the free parameter g increases. As a result, the minimum required energy for the creation of such BHs in the present experimental attempts at the LHC might be larger. This may reduce the possibility for the formation and detection of BHs in TeV-scale collisions at particle colliders.

Acknowledgments

The authors thank to C. Bambi for valuable suggestions.

References

[1] See for instance, S. W. Hawking and G. Ellis, *The Large Scale Structure of Space-Time*, Cambridge University Press, Cambridge, 1973

[2] See for a review, S. Ansoldi, [arXiv:0802.0330]

[3] J. M. Bardeen, in Conference Proceedings of GR5 (Tbilisi, USSR, 1968), p. 174

[4] S. A. Hayward, Phys. Rev. Lett. **96**, 031103 (2006), [arXiv:gr-qc/0506126]

[5] J. C. S. Neves and A. Saa, Phys. Lett. B **734**, 44 (2014), [arXiv:1402.2694]

[6] K. Lin, J. Li and S. Yang, Int. J. Theor. Phys. **52**, 3771 (2013)

[7] G. Abbas and U. Sabiullah, Astrophys. Space Sci. **352**, 769 (2014), [arXiv:1406.0840]

[8] U. Debnath, Eur. Phys. J. C **75**, 129 (2015), [arXiv:1503.01645]

[9] B. Pourhassan, M. Faizal and Ujjal Debnath, Eur. Phys. J. C **76**, 145 (2016), [arXiv:1603.01457]

[10] M. Azreg-Aïnou, Phys. Rev. D **90**, 064041 (2014), [arXiv:1405.2569]

[11] V. P. Frolov, JHEP **05**, 49 (2014), [arXiv:1402.5446]

[12] E. O. Kahya, M. Khurshudyan, B. Pourhassan, R. Myrzakulov and A. Pasqua, Eur. Phys. J. C **75**, 43 (2015), [arXiv:1402.2592]

[13] T. D. Lorenzo, C. Pacilioy, C. Rovelli and S. Speziale, Gen. Rel. Grav. **47**, 41 (2015), [arXiv:1412.6015]

[14] T. D. Lorenzo, A. Giusti and S. Speziale, Gen. Rel. Grav. **48**, 31 (2016), [arXiv:1510.08828]

[15] P. Nicolini, A. Smailagic and E. Spallucci, Phys. Lett. B **632**, 547 (2006), [arXiv:gr-qc/0510112]

[16] S. Ansoldi, P. Nicolini, A. Smailagic and E. Spallucci, Phys. Lett. B **645**, 261 (2007), [arXiv:gr-qc/0612035]

[17] K. Nozari and S. H. Mehdipour, Class. Quant. Grav. **25**, 175015 (2008), [arXiv:0801.4074]

[18] See for a review, P. Nicolini, Int. J. Mod. Phys. A **24**, 1229 (2009), [arXiv:0807.1939]

[19] S. H. Mehdipour, Phys. Rev. D **81**, 124049 (2010), [arXiv:1006.5215]

[20] P. Chen, Y. C. Ong and D. H. Yeom, Phys. Rep. **603**, 1 (2015), [arXiv:1412.8366]

[21] E. T. Newman and A. I. Janis, J. Math. Phys. **6**, 915 (1965)

[22] C. Bambi and L. Modesto, Phys. Lett. B **721**, 329 (2013), [arXiv:1302.6075]

[23] S. P. Drake and P. Szekeres, Gen. Rel. Grav. **32**, 445 (2000), [arXiv:gr-qc/9807001]

[24] L. Modesto and P. Nicolini, Phys. Rev. D **82**, 104035 (2010), [arXiv:1005.5605]

[25] I. Arraut, D. Batic and M. Nowakowski, J. Math. Phys. **51**, 022503 (2010), [arXiv:1001.2226]

[26] A. F. Ali, Phys. Rev. D **89**, 104040 (2014), [arXiv:1402.5320]

[27] A. F. Ali, M. Faizal and M. M. Khalil, Phys. Lett. B **743**, 295 (2015), [arXiv:1410.4765]

[28] A. F. Ali, M. Faizal and M. M. Khalil, Nucl. Phys. B **894**, 341 (2015), [arXiv:1410.5706]

[29] G. Amelino-Camelia, J. Ellis, N. E. Mavromatos and D. V. Nanopoulos, Int. J. Mod. Phys. A **12**, 607 (1997), [arXiv:hep-th/9605211]

[30] S. H. Mehdipour and M. H. Ahmadi, [arXiv:1604.06272]